Contribution from the Department of Inorganic Chemistry,
The University of Sydney, NSW 2006, Australia

Comparisons of π Bonding and Hydrogen Bonding in Isomorphous Compounds: $[M(NH_3)_5Cl]Cl_2$ (M = Cr, Co, Rh, Ir, Ru, Os)

Trevor W. Hambley* and Peter A. Lay*

Received May 8, 1986

The crystal and molecular structures of $[M(NH_3)_5Cl]Cl_2$ (M = Ir, Os, Cr) have been determined, and that with M = Ru has been redetermined. They are isomorphous with the known structures for M = Co and Rh (orthorhombic, space group *Pnma*, $Z = 4$). The cell parameters and bond lengths for the structures are as follows: for Cr, $a = 13.441$ (3) Å, $b = 10.504$ (2) Å, $c = 6.755$ (1) Å, Cr–Cl = 2.327 (1) Å, Cr–N(av) = 2.074 Å; for Ru, $a = 13.418$ (3) Å, $b = 10.501$ (2) Å, $c = 6.777$ (1) Å, Ru–Cl = 2.346 (1) Å, Ru–N(av) = 2.103 Å; for Os, $a = 13.393$ (5) Å, $b = 10.520$ (2) Å, $c = 6.774$ (1) Å, Os–Cl = 2.369 (2) Å, Os–N(av) = 2.113 Å; for Ir, $a = 13.393$ (1) Å, $b = 10.483$ (2) Å, $c = 6.768$ (1) Å, Ir–Cl = 2.371 (2) Å, Ir–N(av) = 2.088 Å. Final *R* values are 0.023, 0.020, 0.021, and 0.027, respectively, for the Cr, Ru, Os, and Ir complexes. In the isomorphous series M = Co, Rh, Ir, Ru, Os, and Cr π bonding in the M–Cl bond is observed to be more important for the d^3 and the d^5 ions than for the d^6 ions. The strength of hydrogen bonding between the ammine hydrogens and the chloride anions increases with decreasing M–N bond lengths, while the strength of the intercomplex hydrogen bonding increases with increasing M–Cl bond lengths.

Introduction

The compounds $[M(NH_3)_5Cl]Cl_2$, M = Ru, Os exhibit some interesting magnetic and spectroscopic properties.[1,2] For instance, the ruthenium ions in $[Ru(NH_3)_5Cl]Cl_2$ become antiferromagnetically coupled to their nearest neighbors at ~0.5 K.[1] This has been attributed to the extensive hydrogen-bonding network that exists in the lattice.[1,3] Similarly, the magnetic circular dichroism (MCD) spectra of $[Os(NH_3)_5Cl]Cl_2$, in the region of the transitions brought about by spin–orbit coupling, show unusual behavior at temperatures approaching absolute zero.[2] Such anomalous behavior was not apparent in other salts of $[Os(NH_3)_5Cl]^{2+}$ and was possibly due to a phenomenon similar to that giving rise to the antiferromagnetic coupling in $[Ru(NH_3)_5Cl]Cl_2$.[2] Similarly, lattice effects on the electron resonance spectra of $[Cr(NH_3)_5Cl]Cl_2$ doped into other $[M(NH_3)_5Cl]Cl_2$ salts have been the subject of exhaustive studies.[4] In order to investigate these factors further, it was desirable to undertake X-ray crystallographic analyses of the Os(III) and Cr(III) complexes.

The isomorphous series, $[M(NH_3)_5Cl]Cl_2$, is also interesting from the point of view of examining the strength of both hydrogen bonding and π bonding as a function of the metal ion. Few systematic studies of this type appear to have been undertaken. One example is the $[M(en)_3]Cl_3{\cdot}3H_2O$ system, where variations in hydrogen bonding with the nature of the metal ion have been studied in detail.[5] Recently, the structures of *cis*-$[Ru(bpy)_2Cl_2]Cl{\cdot}2H_2O$ and *cis*-$[Ru(bpy)_2Cl_2]{\cdot}3.5H_2O$ have been determined, and they revealed a shortening of the Ru–Cl bond in going from d^6 Ru(II) to d^5 Ru(III), while the Ru–N(av) bond lengthened.[6] However, bpy is a π-acid while Cl^- is a π-base, so that it is difficult to delineate the individual contributions to π bonding as a function of the electronic configuration. Furthermore, the two structures are not isomorphous, leading to an uncertainty as to the effects of different packing forces on the observed bond lengths. By contrast, the complexes $[M(NH_3)_5Cl]Cl_2$ are ideal for examining the variations in π bonding, both in going down a group and with a change in the electronic configuration, because the M–N(av) σ-bond length acts as internal standard.

The structures of $[Co(NH_3)_5Cl]Cl_2$[7] and $[Rh(NH_3)_5Cl]Cl_2$[8] have both been determined precisely, and the complexes crystallize in the space group *Pnma*. This was consistent with early studies, which showed that the structures with M = Cr, Co, Rh, and Ir were isomorphous.[9] In this study, the structures of $[Cr(NH_3)_5Cl]Cl_2$, $[Os(NH_3)_5Cl]Cl_2$, and $[Ir(NH_3)_5Cl]Cl_2$ have been determined, and the structure of $[Ru(NH_3)_5Cl]Cl_2$ has been redetermined.

Experimental Section

$[Ru(NH_3)_6]Cl_3$, OsO_4, and K_2IrCl_6 were obtained from Johnson Matthey. $[Ru(NH_3)_5Cl]Cl_2$,[10,11] $[Os(NH_3)_5Cl]Cl_2$,[12,13] $[Ir(NH_3)_5Cl]Cl_2$,[14] $[Ir(NH_3)_5(OSO_2CF_3)](CF_3SO_3)_2$,[15] and $[Cr(NH_3)_5Cl]Cl_2$[16] were prepared by published methods.

Red crystals of $[Cr(NH_3)_5Cl]Cl_2$ were grown from aqueous NaCl/HCl by a method similar to that reported previously.[17] Crystals of $[M(NH_3)_5Cl]Cl_2$ (M = Ru, Os) were obtained by slow cooling (from 100 °C to room temperature) of dilute aqueous HCl solutions of the complexes. For M = Ir, the crystals were best grown as follows. $[Ir(NH_3)_5(OSO_2CF_3)](CF_3SO_3)_2$ was dissolved in boiling water to which sufficient 36% HCl was added to produce a 0.2 M HCl solution. The resultant solution was allowed to cool slowly to room temperature, yielding the colorless crystals used in this study.

Crystallography

Lattice parameters were determined by a least-squares fit to the setting angles of 25 independent reflections. Crystal data collection parameters are listed in Table I.

The structures were refined by using the published coordinates[7] for the cobalt complex as a starting point. Hydrogen atoms were observed in the ruthenium structure, and for the other complexes they were included at comparable sites. The hydrogen atoms were constrained so that there was a tetrahedral geometry about the nitrogen atoms and an N–H distance of 0.91 Å. After addition of the hydrogen atoms, full-matrix least-squares refinement was continued until all shifts were less than 0.05σ.

Programs used were SUSCAD[18] for data reduction, ABSORB[18] for absorption corrections, SHELX 76[19] for refinement and ORTEP[20] for plotting.

---

(1) Carlin, R. L.; Burriel, R.; Seddon, K. R.; Crisp., R. I. *Inorg. Chem.* **1982**, *21*, 4337–4338.

(2) Ferguson, J.; Krausz, E. R.; Lay, P. A.; Maeder, M., to be submitted for publication.

(3) Prout, C. K.; Powell, H. M. *J. Chem. Soc.* **1962**, 137–140.

(4) Garrett, B. B.; Holbrook, M. T.; Stanko, J. A. *Inorg. Chem.* **1977**, *16*, 1159–1163 and references therein.

(5) Smolenaers, P. J.; Beattie, J. K.; Hutchinson, N. D. *Inorg. Chem.* **1981**, *20*, 2202–2206 and references therein.

(6) bpy = 2,2′-bipyridine: Eggleston, D. S.; Goldsby, K. A.; Hodgson, D. J.; Meyer, T. J. *Inorg. Chem.* **1985**, *24*, 4573–4580.

(7) Messmer, G. G.; Amma, E. L. *Acta Crystallogr., Sect. B.; Struct. Crystallogr. Cryst. Chem.* **1968**, *B24*, 417–422.

(8) Evans, R. S.; Hopcus, E. A.; Bordner, J.; Schreiner, A. F. *J. Cryst. Mol. Struct.* **1973**, *3*, 235–245.

(9) West, C. D. *Z. Kristallogr., Kristallgeom., Kristallphys., Kristallchem.* **1935**, *91*, 181–186.

(10) Vogt, L. H., Jr.; Katz, J. L.; Wiberley, S. E. *Inorg. Chem.* **1965**, *4*, 1157–1163.

(11) Lawrance, G. A.; Lay, P. A.; Sargeson, A. M.; Taube, H. *Inorg. Synth.* **1986**, *24*, 257–263.

(12) Allen, A. D.; Stevens, J. R. *Can. J. Chem.* **1973**, *51*, 92–98.

(13) Lay, P. A.; Magnuson, R. H.; Taube, H. *Inorg. Synth.* **1986**, *24*, 269–279.

(14) Hendrickson, D. N.; Jolly, W. L. *Inorg. Chem.* **1970**, *9*, 1197–1201.

(15) Dixon, N. E.; Lawrance, G. A.; Lay, P. A.; Sargeson, A. M. *Inorg. Chem.* **1984**, *23*, 2940–2947. Lay, P. A.; Sargeson, A. M. *Inorg. Synth.* **1986**, *24*, 263–269.

(16) Schlessinger, G. *Inorg. Synth.* **1960**, *6*, 138–141.

(17) Zinato, E.; Lindholm, R.; Adamson, A. W. *J. Inorg. Nucl. Chem.* **1969**, *31*, 449–453.

(18) Guss, J. M. "SUSCAD and ABSORB, Data Reduction and Absorption Correction for the CAD4"; University of Sydney, 1976.

(19) Sheldrick, G. M. "Shelx 76, Program for Crystal Structure Determination"; University of Cambridge, 1976.

0020-1669/86/1325-4553$01.50/0

Table I. Crystal Data for $[M(NH_3)_5Cl]Cl_2$ (M = Cr, Ru, Os, Ir)

	Cr	Ru	Os	Ir
color	red	orange	yellow	pale yellow
cryst syst	orthorhombic	orthorhombic	orthorhombic	orthorhombic
space group	*Pnma*	*Pnma*	*Pnma*	*Pnma*
a, Å	13.441 (3)	13.418 (3)	13.393 (5)	13.393 (1)
b, Å	10.504 (2)	10.501 (2)	10.520 (2)	10.483 (2)
c, Å	6.755 (1)	6.777 (1)	6.774 (1)	6.768 (1)
V, Å^3	956.4	954.9	954.4	950.3
D_{calcd}, g cm^{-3}	1.691	2.035	2.656	2.682
empirical formula	$Cl_3CrH_{15}N_5$	$Cl_3H_{15}N_5Ru$	$Cl_3H_{15}N_5Os$	$Cl_3H_{15}IrN_5$
fw	243.5	292.6	381.7	383.7
Z	4	4	4	4
F(000), electrons	488	580	708	712
abs coeff, cm^{-1}	18.84	23.30	174.10	147.20
habit	plates	prismatic	plates	octahedral
dimens, mm	0.06 × 0.12 × 0.10	0.18 × 0.14 × 0.12	0.13 × 0.13 × 0.03	0.11 × 0.11 × 0.10
absorpn factors	1.15, 1.12	1.37, 1.28	3.57, 1.99	3.92, 3.16
temp, K	294	294	294	294
diffractometer	*a*	*a*	*a*	*a*
radiation	*b*	*b*	*b*	*b*
monochromator	graphite	graphite	graphite	graphite
scan model	ω–θ	ω–θ	ω–$^4/_3\theta$	ω–θ
scan width, deg	1.0 + 0.35(tan θ)	1.6 + 0.35(tan θ)	1.2 + 0.35(tan θ)	1.0 + 0.35(tan θ)
horiz counter apert, mm	2.40 + 0.5(tan θ)	2.40 + 0.5(tan θ)	2.40 + 0.5(tan θ)	2.40 + 0.5(tan θ)
2θ range, deg	1.0–50.0	1.0–50.0	1.0–50.0	1.0–50.0
no. of reflcns measd ($+h,+k,+l$)	801	843	823	849
no. of reflcns used ($I > 2.5\sigma(I)$)	675	778	714	789
R	0.023	0.020	0.021	0.027
R_w	0.027	0.023	0.022	0.029
$w = g/(\sigma^2F_o + kF_o^2)$: g; k	1.0; 1.7 × 10^{-3}	1.01; 0.36 × 10^{-3}	0.96; 0.1 × 10^{-3}	1.02; 1.2 × 10^{-3}

[a] Enraf-Nonius CAD4-F, four circle. [b] Mo Kα; λ = 0.71069 Å.

Table II. Positional Parameters (×10^4) for $[Cr(NH_3)_5Cl]Cl_2$

	x	y	z
Cr(1)	1026 (1)	2500	1787 (1)
Cl(1)	-279 (1)	2500	-466 (1)
Cl(2)	3525 (1)	10 (1)	1632 (1)
N(1)	2199 (3)	2500	3768 (6)
N(2)	2058 (3)	2500	-501 (6)
N(3)	1027 (2)	527 (2)	1781 (4)
N(4)	41 (3)	2500	4141(5)

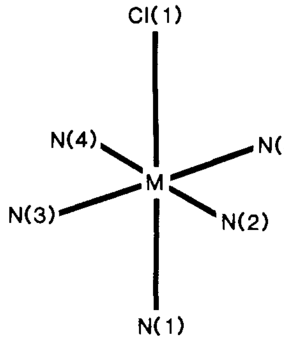

Figure 1. Numbering system used for the $[M(NH_3)_5Cl]^{2+}$ ions.

Table III. Positional Parameters (×10^4) for $[Ru(NH_3)_5Cl]Cl_2$

	x	y	z
Ru(1)	1029 (1)	2500	1802 (1)
Cl(1)	-288 (1)	2500	-470 (2)
Cl(2)	3518 (1)	12 (1)	1633 (1)
N(1)	2210 (3)	2500	3824 (7)
N(2)	2063 (3)	2500	-522 (6)
N(3)	1027 (2)	495 (3)	1798 (4)
N(4)	19 (3)	2500	4185 (6)

Table IV. Positional Parameters (×10^4) for $[Os(NH_3)_5Cl]Cl_2$

	x	y	z
Os(1)	1027 (1)	2500	1794 (1)
Cl(1)	-305 (2)	2500	-502 (4)
Cl(2)	3515 (1)	13 (2)	1618 (3)
N(1)	2218 (7)	2500	3817 (13)
N(2)	2061 (7)	2500	-581 (14)
N(3)	1014 (4)	491 (6)	1790 (9)
N(4)	2 (7)	2500	4157 (12)

Table V. Positional Parameters (×10^4) for $[Ir(NH_3)_5Cl]Cl_2$

	x	y	z
Ir(1)	1036 (1)	2500	1804 (1)
Cl(1)	-302 (2)	2500	-485 (3)
Cl(2)	3514 (1)	18 (2)	1602 (2)
N(1)	2207 (6)	2500	3796 (14)
N(2)	2044 (7)	2500	532 (12)
N(3)	1020 (4)	498 (7)	1779 (8)
N(4)	14 (6)	2500	4151 (13)

Scattering factors and anomalous dispersion terms were taken from ref 21.

Results

Crystallographic data for the complexes $[M(NH_3)_5Cl]Cl_2$ (M = Cr, Ru, Os, Ir) are contained in Table I. All complexes crystallized in the space group *Pnma* and possessed an extended hydrogen-bonding network involving the ammine hydrogens and both ionic and coordinated Cl$^-$. The numbering system used for the $[M(NH_3)_5Cl]^{2+}$ ions is illustrated in Figure 1, while the hydrogen-bonding network is illustrated in Figure 2 (for $[Os(NH_3)_5Cl]Cl_2$). The other structures are so similar that we have not included separate diagrams. Positional parameters and estimated standard deviations for M = Cr, Ru, Os, and Ir are contained in Tables II–V, respectively. Tables VI and VII contain, respectively, bond distances and angles within the $[M(NH_3)_5Cl]^{2+}$ ions (M = Co,[7] Rh,[8] Ir, Ru, Os, Cr).

The M–N(av) distances are typical for amine complexes of Cr(III),[22-25] Ru(III),[3,26-28] and Os(III).[29,30] The Ir–N(av) bond

---

[20] Johnson, C. K. "ORTEP", Report ORNL-3794; Oak Ridge National Laboratories: Oak Ridge, TN, 1965.

[21] *International Tables for X-ray Crystallography*; Kynoch: Birmingham, England, 1974; Vol. 4, p 99.

[22] Wieghardt, K.; Weiss, J. *Acta Crystallogr., Sect. B: Struct. Crystallogr. Cryst. Chem.* **1972**, *B28*, 529–534.

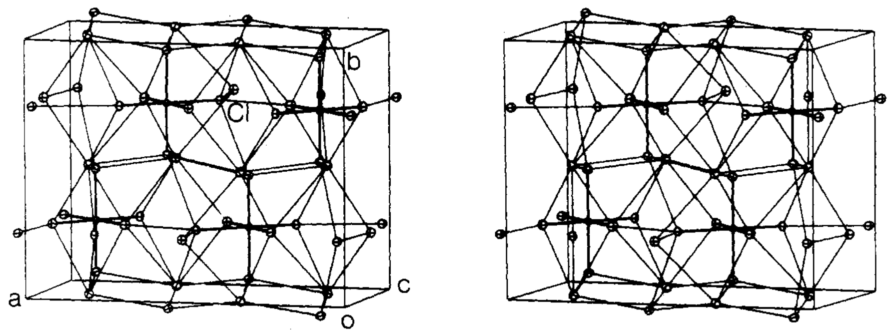

Figure 2. Extended hydrogen-bonding array in the unit cell of $[Os(NH_3)_5Cl]Cl_2$. N···Cl contacts are indicated by the light lines, while the metal–ligand bonds are indicated by the heavy lines.

Table VI. Bond Distances (Å) for $[M(NH_3)_5Cl]^{2+}$ (M = Cr, Co, Rh, Ir, Ru, Os)

bond	M = Cr	M = Co[a]	M = Rh[b]	M = Ir	M = Ru	M = Os
M–Cl	2.327 (1)	2.286 (2)	2.356 (1)	2.371 (2)	2.346 (1)	2.369 (2)
M–N(1)	2.070 (4)	1.964 (6)	2.051 (4)	2.068 (8)	2.096 (4)	2.103 (8)
M–N(2)	2.081 (3)	1.978 (6)	2.061 (4)	2.079 (8)	2.100 (4)	2.123 (9)
M–N(3)	2.073 (2)	1.962 (4)	2.057 (2)	2.099 (7)	2.105 (3)	2.115 (6)
M–N(4)	2.072 (3)	1.998 (6)	2.052 (4)	2.097 (8)	2.108 (4)	2.110 (9)
M–N(av)[c]	2.074	1.973	2.056	2.088	2.103	2.113

[a] Reference 7. [b] Reference 8. Note that the atomic numbering system has been altered from the original reference so that all of the structures have the same numbering system. [c] The average includes a weighting factor of 2 for the two M–N(3) bonds.

Table VII. Bond Angles (deg) for $[M(NH_3)_5Cl]^{2+}$ (M = Cr, Co, Rh, Ir, Ru, Os)

angle[a]	M = Cr	M = Co[b]	M = Rh[c]	M = Ir	M = Ru	M = Os
Cl(1)–M–N(1)	179.4 (1)	179.7 (2)	179.5 (1)	179.9 (1)	179.8 (1)	179.6 (2)
Cl(1)–M–N(2)	90.8 (1)	89.4 (2)	89.7 (1)	89.6 (3)	90.3 (1)	89.6 (2)
Cl(1)–M–N(3)	89.9 (1)	89.0 (1)	89.3 (1)	89.2 (1)	89.9 (1)	90.4 (2)
Cl(1)–M–N(4)	91.3 (1)	90.3 (2)	90.7 (1)	90.1 (2)	91.1 (1)	90.4 (2)
N(1)–M–N(2)	88.6 (2)	90.9 (3)	89.9 (1)	90.2 (4)	89.5 (2)	90.0 (4)
N(1)–M–N(3)	90.1 (1)	91.0 (1)	90.7 (1)	90.8 (1)	90.1 (1)	90.4 (2)
N(1)–M–N(4)	89.3 (2)	89.4 (3)	89.8 (1)	90.1 (4)	89.2 (2)	90.0 (4)
N(2)–M–N(3)	89.9 (1)	90.2 (1)	89.9 (1)	90.0 (1)	90.0 (1)	90.3 (2)
N(2)–M–N(4)	177.9 (2)	179.8 (3)	179.7 (1)	179.7 (2)	178.6 (2)	180.0 (1)
N(3)–M–N(3)$^{-4}$	177.3 (1)	178.0 (1)	178.5 (1)	177.5 (2)	179.8 (1)	179.0 (1)
N(3)–M–N(4)	90.1 (1)	89.8 (1)	90.1 (1)	90.0 (1)	90.0 (1)	89.7 (2)
Cl(1)–M–N(av)[d]	90.5	89.4	89.8	89.5	90.3	90.2

[a] The superscript −4 denotes the position x, $y - {}^1/_2$, z in the unit cell. [b] From ref 7. [c] From ref 8. See footnote *b* from Table VI. [d] Average *cis*-[Cl(1)–M–N] bond angle, which includes a weighting factor of 2 for the two Cl(1)–M–N(3) bond angles.

Table VIII. Close Contacts (Å) between Ammine Ligands and the Chlorine Atoms in $[M(NH_3)_5Cl]Cl_2$ (M = Cr, Co, Rh, Ir, Ru, Os)

contact[a,b]	M = Cr	M = Co[c]	M = Rh[d]	M = Ir	M = Ru	M = Os
N(1)···Cl(2)	3.480	3.448	3.455	3.469	3.480	3.477
N(2)···Cl(2)	3.580	3.550	3.560	3.568	3.573	3.587
N(3)···Cl(2)	3.403	3.375	3.373	3.379	3.383	3.389
N(4)···Cl(2)^{2}	3.357	3.330	3.341	3.326	3.344	3.330
N(1)···Cl(2)$^{-2}$	3.415	3.370	3.392	3.392	3.397	3.401
N(2)···Cl(2)$^{-2}$	3.367	3.346	3.354	3.360	3.360	3.346
N(4)···Cl(2)$^{-2}$	3.676	3.612	3.663	3.689	3.683	3.705
N(3)···Cl(2)^{3}	3.389	3.351	3.363	3.367	3.375	3.373
N(3)···Cl(2)$^{-3}$	3.572	3.545	3.566	3.567	3.566	3.552
N(3)···Cl(1)$^{-1}$	3.451	3.491	3.433	3.401	3.417	3.402
N(1)···Cl(1)^{2}	3.578	3.610	3.530	3.526	3.536	3.507
N···Cl(1)(av)[e]	3.493	3.531	3.465	3.443	3.457	3.437
N···Cl(2)(av)[f]	3.467	3.433	3.447	3.453	3.457	3.456

[a] The first nine entries are hydrogen bonding between the complex and counterions, while the next two are hydrogen bonding between complex ions. [b] The superscripts refer to the following positional parameters: (−1) $-x, -y, -z$; (2) ${}^1/_2 + x, {}^1/_2 - y, {}^1/_2 - z$; (−2) ${}^1/_2 - x, {}^1/_2 + y, {}^1/_2 + z$; (3) ${}^1/_2 - x, -y, {}^1/_2 + z$; (−3) $x, {}^1/_2 - y, z$. [c] Calculated from the positional parameters contained in ref 7. [d] Calculated from the positional parameters contained in ref 8. [e] Average N···Cl contact between the complexes, which is weighted to take account for the two equivalent N(3)···Cl(1) contacts per complex. [f] Average N···Cl contact between the complex cation and the anions, which is weighted to take account of the three pairs of equivalent N(3)···Cl(2) contacts per complex.

length of 2.088 Å is slightly longer than those reported in the structure of *cis*-$[Ir(en)_2Cl_2]Cl$ (2.01–2.06 Å),[31] but the latter structure determination was much less precise. Similarly, the M–Cl distances are typical of other M–Cl distances in Cr(III),[32,33]

---

(23) Raymond, K. N.; Meek, D. W.; Ibers, J. A. *Inorg. Chem.* **1968**, *7*, 1111–1117.

(24) Clegg, W. *Acta Crystallogr., Sect. B: Struct. Crystallogr. Cryst. Chem.* **1978**, *B34*, 3328–3330.

(25) Clegg, W. *Acta Crystallogr., Sect. B: Struct. Crystallogr. Cryst. Chem.* **1976**, *B32*, 2907–2909.

(26) Hambley, T. W.; Lawrance, G. A. *Aust. J. Chem.* **1984**, *37*, 435–441 and references therein.

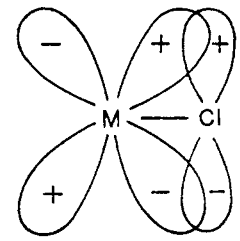

Figure 3. Interaction of a d_{xz}(M) orbital with the $3p_x$(Cl) orbital or a d_{yz}(M) orbital with the $3p_y$(Cl) orbital in $[M(NH_3)_5Cl]^{2+}$.

Ru(III),[6,26,27,34,35] and Ir(III)[31,36] complexes.

There are two sets of hydrogen-bonding networks, one involving the ammine ligands and the chloride counterion and one involving the chloro ligand and the ammine ligands of adjacent complexes (Table VIII). For the former, there is a clear trend toward shorter contacts as the value of M–N(av) decreases, while for the latter, there are shorter contacts with increasing M–Cl bond distances. It has been assumed that contacts between the ammine nitrogen atoms and the chlorine (chloro) atoms which are less than 3.7 Å correspond to hydrogen bonds, because this is the sum of the van der Waals radii of N (1.7 Å) and Cl (2.0 Å).[37]

Discussion

The isomorphous series of compounds $[M(NH_3)_5Cl]Cl_2$ have complex ions that possess a mirror plane bisecting Co, Cl(1), N(1), N(2), and N(4), giving two equivalent NH_3 ligands containing the N(3) atoms. The packing of the anions and cations are such that the ionic chlorides, Cl(2), occur on the corners of a cube surrounding the complex ion, with the chloro ligand, Cl(1), protruding into the middle of one face of this cube. These geometric considerations are important to the ensuing discussions.

π Bonding. The $3p_x$ and $3p_y$ orbitals of the sp-hybridized chloro ligands can interact with the nonbonding d orbitals of e symmetry (assuming a C_{4v} point group) as shown in Figure 3. In the d^6 series of complexes, M = Co, Rh, Ir, both the nonbonding metal d and the ligand 3p(Cl) orbitals are filled, so that such an overlap would not lead to a bonding interaction (unless the next lowest energy of empty metal d orbitals were involved). However, for the d^3 complex M = Cr and the d^5 complexes M = Ru and Os, the overlap depicted in Figure 3 would lead to a net bonding interaction, as there are four electrons in a degenerate bonding set of 3p(Cl) orbitals, but only one and three electrons in the nonbonding d(M) orbitals of e symmetry, respectively, for the d^3 and d^5 electronic configurations.[38] Therefore, we would expect to see a shortening of the M–Cl bond in the d^3 and d^5 complexes as compared to the d^6 complexes. Such effects are seen clearly when we compare the structures of the d^3 and the d^5 complexes with the d^6 complexes of the same transition-metal row. The effect is most pronounced in the second row, where the Ru–N(av) bond is 0.05 Å longer than is the Rh–N(av) bond, but the Ru–Cl bond is 0.010 (2) Å shorter than is the Rh–Cl bond. Clearly, the Ru–Cl bond would be expected to be at least 0.05 Å longer than the Rh–Cl bond, in the absence of any π bonding. Similarly, the Os–N(av) bond is 0.03 Å longer than is the Ir–N(av) bond, but the Os–Cl bond is equal to (0.002 (4) Å) the Ir–Cl bond. Finally, the Cr–N(av) bond is 0.10 Å longer than is the Co–N(av) bond, but the Cr–Cl bond is only 0.041 Å longer than the Co–Cl bond. Table IX illustrates the differences between the d^3, d^5, and d^6 ions further, where the Ru–Cl bond is clearly shortened in comparison to the Ru–N(av) bond when compared with those for the d^6 ions. The shortening is even more pronounced than is indicated by the values contained in Table IX, because the M–Cl bonds are inherently longer than the M–N(av) bonds, due to the larger radius of Cl as opposed to N. Hence, the differences in the M–Cl bond distances, Δd(M–Cl), should be greater (and not smaller) than the differences in the M–N(av) bond lengths, Δd(M–N(av)), in the absence of π bonding. In addition, the $[Pt(NH_3)_5Cl]^{3+}$ ion in the structure of $[Pt(NH_3)_5Cl]Cl_3{\cdot}H_2O$[39] follows the trends observed for the other d^6 ions (Table IX), even though the structure is not isomorphous because the complex has an overall charge of 3+. Similarly, the structure of $[Co(NH_3)_5Cl]SiF_6$,[40] while less precise than that of $[Co(NH_3)_5Cl]Cl_2$,[7] shows analogous trends in the bond lengths within the $[Co(NH_3)_5Cl]^{2+}$ ion, (Table IX). The longer Co–N(av) and Co–Cl bonds found in $[Co(NH_3)_5Cl]SiF_6$ may be due to one or both of the factors of the lower precision of this structure or different hydrogen-bonding interactions. Clearly, the structures of $[Pt(NH_3)_5Cl]Cl_3{\cdot}H_2O$ and $[Co(NH_3)_5Cl]SiF_6$, show that the trends observed in the metal–chloro bonds are not due to packing forces, but are inherent to the M–Cl bonding within the complex.

Table IX. Differences in Bond Lengths in $[Ru(NH_3)_5Cl]Cl_2$ As Compared with Bond Lengths in $[M(NH_3)_5Cl]Cl_2$ (M = Cr, Co, Rh, Ir, Os) and $[Pt(NH_3)_5Cl]Cl_3{\cdot}H_2O$

	Pt[c]	Cr	Co[d]	Rh[e]	Ir	Os
Δd(M–N(av)),[a] Å	0.10	0.03	0.13(0.10)	0.05	0.02	−0.01
Δd(M–Cl),[b] Å	0.05	0.019	0.06(0.04)	−0.010	−0.025	−0.023

[a] d[Ru–N(av)] − *d*[M–N(av)]. [b] *d*[Ru–Cl] − *d*[M–Cl]. [c] Calculated from ref 39. [d] Calculated from ref 7; values calculated from $[Co(NH_3)_5Cl]SiF_6$[40] distances are given in parentheses. [e] Calculated from ref 8.

The values of Δd(M–Cl) and Δd(M–N(av)) obtained for Os were equal, within experimental error, which indicates that the strength of π bonding is similar in both $[Ru(NH_3)_5Cl]^{2+}$ and $[Os(NH_3)_5Cl]^{2+}$. This contrasts with the behavior observed where the predominant form of π bonding is back-donation of electron density from filled metal d orbitals to a ligand π^* orbital, as in the complexes $[(NH_3)_5M^{III}(pz)M^{III}(NH_3)_5]Cl_6{\cdot}2H_2O$. Here, the Os–N(pz) bond was shortened considerably in comparison to the other Os–N bonds, while the Ru–N(pz) bond was the longest (within experimental error) in the Ru structure.[28,29,41] This was attributed to Os(III) being much better at π back-bonding than is Ru(III)[29] and is supported by a growing body of chemical evidence. For instance, the greater kinetic stability of $[(NH_3)_5OsN_2Os(NH_3)_5]Cl_6$, to decomposition,[42] and the lower susceptibility of $[Os(NH_3)_5(NCCH_3)]^{3+}$ toward nucleophilic attack by water,[43] in comparison to the Ru analogues,[44,45] suggests greatly

---

(27) Bottomley, F. *Can. J. Chem.* **1977**, *55*, 2788–2791.

(28) pz = pyrazine: Fürholz, U.; Joss, S.; Bürgi, H. B.; Ludi, A. *Inorg. Chem.* **1985**, *24*, 943–948 and references therein.

(29) Bino, A.; Lay, P. A.; Taube, H.; Wishart, J. F. *Inorg. Chem.* **1985**, *24*, 3969–3971.

(30) en = 1,2-ethanediamine: Lay, P. A.; McLaughlin, G. M.; Sargeson, A. M., submitted for publication in *Aust. J. Chem.*

(31) Shvelashvili, A. E.; Kvitashvili, A. I.; Kandelaki, M. N.; Mikeladze, E. A. *Soobshch. Akad. Nauk Gruz. SSR* **1975**, *77*, 361–364. *Chem. Abstr.* **1975**, *83*, 51299a.

(32) Ooi, S.; Komiyama, Y.; Kuroya, H. *Bull. Chem. Soc. Jpn* **1960**, *33*, 354–357.

(33) Hardcastle, K. I.; Skovlin, D. O.; Eidawad, A.-H. *J. Chem. Soc., Chem. Commun.* **1975**, 190.

(34) Krentzien, H. J.; Clarke, M. J.; Taube, H. *Bioinorg. Chem.* **1975**, *4*, 143–151.

(35) McGuiggan, M. F.; Pignolet, L. H. *Cryst. Struct. Commun.* **1981**, *10*, 1227–1232.

(36) Bonnet, J.-J.; Jeannin, Y. *J. Inorg. Nucl. Chem.* **1973**, *35*, 4103–4111.

(37) Allinger, N. L. *Adv. Phys. Org. Chem.* **1976**, *13*, 1–82.

(38) Although the symmetry of the ions is no longer C_{4v} in the lattice, the distortions are small and the arguments for the idealized C_{4v} geometry are still relevant.

(39) Bokij, G. B.; Popova, L. A. *Dokl. Akad. Nauk SSSR* **1949**, *67*, 73–76. See also: *Structure Reports*; Wilson, A. J. C., Barrett, J. M., Robertson, J. M., Eds.; N. V. A. *Oostheok*'s, MIJ: Utrecht, the Netherlands, 1949: Vol. 12, pp 225–226.

(40) Stanko, J. A.; Paul, I. C. *Inorg. Chem.* **1967**, *6*, 486–490.

(41) Fürholz, U.; Bürgi, H.-B.; Wagner, F. E.; Stebler, A.; Ammeter, J. H.; Krausz, E.; Clark, R. J. H.; Stead, M. J.; Ludi, A. *J. Am. Chem. Soc.* **1984**, *106*, 121–123.

(42) Lay, P. A.; Magnuson, R. H.; Taube, H.; Ferguson, J.; Krausz, E. R. *J. Am. Chem. Soc.* **1985**, *107*, 2551–2552.

(43) Lay, P. A.; Magnuson, R. H.; Taube, H., to be submitted for publication.

(44) Anderes, B.; Lavallee, D. K. *Inorg. Chem.* **1983**, *22*, 3724–3726 and references therein.

Table X. Differences in Bond Lengths in $[Co(NH_3)_5Cl]Cl_2$ As Compared with Those for the Other d^6 Ions

	Co	Rh	Ir	Pt
Δd(M–N(av)),[a] Å	0	−0.083	−0.115	−0.03
Δd(M–Cl)[b] Å	0	−0.070	−0.085	−0.01

[a] d[Co–N(av)] − d[M–N(av)]. [b] d[Co–Cl] − d[M–Cl].

enhanced π back-bonding in Os(III). These phenomena were rationalized in terms of the greater extension of Os(III) d orbitals (better spatial overlap with the ligand π* orbitals) and the better energy overlap of the Os(III) d orbitals with the ligand π* orbitals than those for Ru(III).[46]

While the spatial overlap factor also favors Os(III) over Ru(III) in π bonding, the energy overlap factor now favors Ru(III) over Os(III). It appears that these factors approximately cancel, resulting in a similar degree of π bonding in $[Ru(NH_3)_5Cl]^{2+}$ and $[Os(NH_3)_5Cl]^{2+}$. It should also be noted that π back-bonding is inherently stronger than π bonding, because of the better spatial overlap of orbitals in the former case.[47] Therefore, any differences between Os and Ru in their π interactions will be more pronounced when considering π back-bonding, as compared to π bonding.

While the contraction of the M–Cl bond due to π bonding is not as great for d^3 Cr as compared to d^5 Ru, it was not possible to compare d^3, d^5, and d^6 complexes in the same row of the transition series. It is likely that the complex $[Mo(NH_3)_5Cl]Cl_2$ would exhibit even stronger π bonding than that observed for $[Ru(NH_3)_5Cl]Cl_2$, if the former complex could be prepared and crystallized. What is clear, is that π bonding in the chromium complex is of the same order of magnitude as that observed in the ruthenium complex, despite the smaller radial extension of the orbitals for chromium.

When the structures of $[Cr(NH_2CH_3)_5Cl]Cl_2$ and $[Co(NH_2CH_3)_5Cl](NO_3)_2$ are compared,[48] the contraction of the M–Cl bond in the d^3 ion is greater than in the analogous pentaammine complexes, but the differences in the two series may be due to the steric requirements of the methylamine ligands.[48,49] This is discussed in more detail elsewhere and has important implications for understanding the mechanisms of substitution reactions of Co(III) and Cr(III).[49]

An increase in π bonding in going from the d^6 to the d^5 or d^3 ions, would cause an increase in the Cl–M–N(cis) bond angles due to increased repulsions between the multiple bond and the single bond, as compared to two single bonds. Such distortions can be quite large, e.g. in *cis*-$[Os(en\text{-}H)_2(en)]Br_2$.[30,50] Indeed, the average value of Cl–M–N(cis) of 89.4° for $[Co(NH_3)_5Cl]Cl_2$ was ~1° less than that for Ru (90.3°), Os (90.2°), or Cr (90.5°). While such effects are small, they are greater than the experimental error, and the other d^6 ions exhibit average bond angles similar to those of Co(III) (Table VII). Therefore, the bond angle data is consistent with the notion of increased π bonding in the d^3 and d^5 ions as compared to the d^6 ions, even if the effect is small.

There are some interesting factors that are apparent when the bond lengths in the d^6 complexes are compared. First, the M–N(av) bond lengths show a change between Rh and Ir which is less than half that between Co and Rh. While the smaller increment in going from Rh to Ir is to be expected due to the effects of lanthanide contraction, it is larger than the difference between Ru and Os. The reason for this difference is not immediately obvious. Secondly, the increase in the M–Cl bond length is less than that in the M–N(av) bond length, which is especially noticeable in Ir (Table X). Again, it is to be expected that the increments in M–Cl should be larger than those in M–N(av) in the absence of π bonding. These results can be explained by π bonding between the lowest energy empty d orbitals (i.e. 4d for Co, 5d for Rh, and 6d for Ir) with the filled $3p_x$ and $3p_y$ orbitals of the chloro ligand. Such π bonding is expected and is found to be weaker than that exhibited for the d^5 ions, because of a much poorer energy overlap. The higher density of states (making the unoccupied d level more accessible) as you go down the group, plus the greater d-orbital extension, favors π bonding in going down the group for the d^6 ions. Like Ir(III), Pt(IV) shows a marked decrease in the M–Cl bond length compared to that expected in the absence of π bonding (Table X).

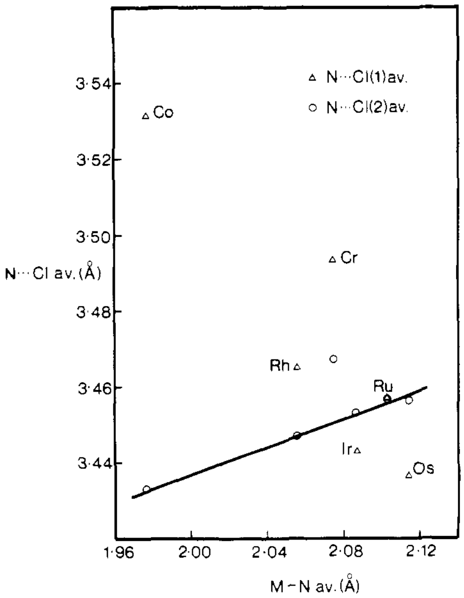

Figure 4. Average M–N bond lengths plotted against average N···Cl contacts for the two types of hydrogen bonds: hydrogen bonds between the Cl^- counterions (N···Cl(1)(av)) and the $[M(NH_3)_5Cl]^{2+}$ complexes (○) and intercomplex hydrogen bonds (N···Cl(2)(av)) (△).

Hydrogen Bonding. For analysis of the overall strength of the hydrogen-bond network, weighted average N···Cl contacts have been examined. These numbers reflect the overall strengths of the intercomplex and complex/anion forces rather than individual strengths of hydrogen bonds. It is apparent from Table VIII and Figure 4, that the hydrogen bonding between the complexes and chloride counterions increases in strength with decreasing M–N bond length (i.e. the weighted average N···Cl(2) contact increases in the order Co < Rh < Ir < Ru ≈ Os). The Cr complex deviates from this behavior, but the cause of this deviation is not clear at present. This implies that the dominant factor influencing the acidity of the N–H bonds and hence the hydrogen-bonding network is the polarizing ability of the central metal ion (i.e. charge: radius ratio). Therefore, the extent of M–Cl π bonding has little effect on the polarization of the N–H bonds. This is supported by the results presented for the isomorphous series (±)-$[M(en)_3]Cl_3{\cdot}3H_2O$, where a slight increase in N···Cl contacts was observed with increasing M–N bond length.[5]

The above results are in contrast with the results obtained for the intercomplex hydrogen bonding, in that the N···Cl(1) distances decreases with increasing M–N distances (Figure 4). Instead, the N···Cl contact distances exhibit changes that are comparable to the changes in the M–Cl distances and show a general decrease with increasing M–Cl bond length (Figure 5). This leads to the conclusion that the charge on the chlorine is the dominant factor. Again, M–Cl π bonding cannot be the source of these trends, as this would tend to decrease the negative charge on the chloro ligands bound to the d^5 ions, leading to weaker hydrogen bonding. Apparently, σ polarization of the Cl^- charge cloud toward the metal ion is more important than are the effects of π bonding.

While the changes in the M–L bond lengths influence the changes in the unit cell parameters, the changes in intercomplex hydrogen bonding are the major contributions. This manifests itself mainly in the *a* and *c* directions, which change by 1.1 and 0.9%, respectively, in the series, which contrasts with an increase

---

(45) Richardson, D. E.; Sen, J. P.; Buhr, J. D.; Taube, H. *Inorg. Chem.* **1982**, *21*, 3136–3140.
(46) Taube, H. *Pure Appl. Chem.* **1979**, *51*, 901–912.
(47) Lay, P. A. *Inorg. Chem.* **1984**, *23*, 4775–4777.
(48) Foxman, B. M. *Inorg. Chem.* **1978**, *17*, 1932–1938.
(49) Lay, P. A. *J. Chem. Soc., Chem. Commun.*, in press.
(50) en-H = 1,2-ethanediaminato(1−): Lay, P. A.; Sargeson, A. M.; Skelton, B. W.; White, A. H. *J. Am. Chem. Soc.* **1982**, *104*, 6161–6164.

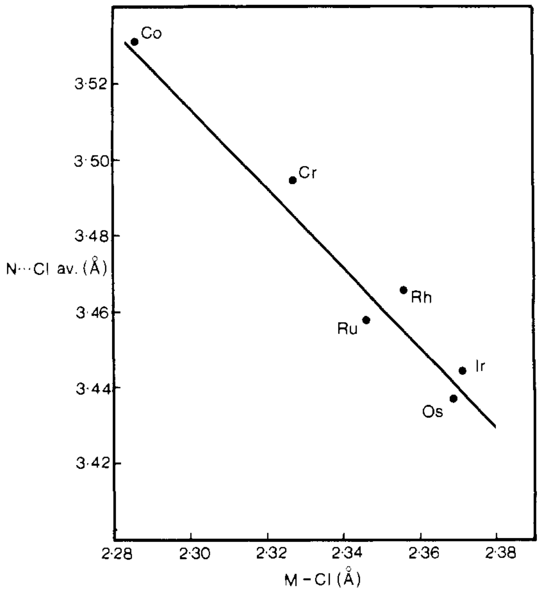

Figure 5. M–Cl bond lengths plotted against the average N···Cl contacts for the intercomplex hydrogen bonds.

in bond lengths of the order of 5–6%. The importance of this contraction, due to hydrogen bonding, is seen in the cell parameters of Ru and Os (Table I), where the *a* parameter for Os is significantly shorter than that for Ru, despite the longer Os–ligand bonds.

The increase along the *b* axis in going from Co to Os is larger (~1.7%), but still much smaller than the increase in average M–L bond lengths. From these results, it would be predicted that the exchange coupling between $[Os(NH_3)_5Cl]^{2+}$ centers should be larger than that observed between the $[Ru(NH_3)_5Cl]^{2+}$ centers,[1] if indeed the coupling occurs via intercomplex hydrogen bonding. This prediction awaits experimental verification at present. However, the postulate that this intercomplex hydrogen bonding provides a pathway for weak exchange coupling of paramagnetic ions and hence unusual magnetic and spectroscopic behavior would appear to be reasonable, since all of the $[M(NH_3)_5Cl]Cl_2$ structures have the same intercomplex hydrogen bonding.

Conclusions

The expected increase in π bonding in M–Cl bonds in going from a d^6 to d^5 or d^3 electronic configuration was observed experimentally. Changes in hydrogen bonding between the complex ions and the counterions are small, but are dominated by polarization of the N–H bonds due to the changes in M–N bond lengths. The intercomplex hydrogen bonds show a much larger variation with the nature of M and their strengths decrease with decreasing M–Cl bond length. Again, this is attributed to an increased polarization of the ligand electron density toward the metal ion as its charge:radius ratio decreases.

Acknowledgment. P.A.L. is grateful for support from the Australian Research Grants Scheme.

Supplementary Material Available: Tables of anisotropic thermal parameters and calculated atomic positions of hydrogen atoms for $[M(NH_3)_5Cl]Cl_2$ (M = Cr, Ru, Os, Ir) (8 pages); tables of observed and calculated structure factors for $[M(NH_3)_5Cl]Cl_2$ (M = Cr, Ru, Os, Ir) (19 pages). Ordering information is given on any current masthead page.

Contribution from the Department of Chemistry,
Washington State University, Pullman, Washington 99164-4630

Crystal Structure of $[(C_2H_5)_4N]_4Cu_4Cl_{12}$, a New Structural Type for a Tetranuclear Copper(II) Halide Complex

R. D. Willett* and Urs Geiser[1]

Received May 29, 1986

The crystal structure of the compound with the empirical formula $(C_2H_5)_4NCuCl_3$ has been determined. The crystals are monoclinic, space group $P2_1/c$, with a = 13.799 (3) Å, b = 11.316 (2) Å, c = 17.883 (3) Å, and β = 106.04 (2)°, with Z = 2. The compound is shown to have the chemical formula $[(C_2H_5)_4N]_4Cu_4Cl_{12}$ and to consist of discrete $(C_2H_5)_4N^+$ cations and $Cu_4Cl_{12}^{4-}$ anions. The centrosymmetric anions contain copper atoms in two distinct coordination geometries: the central pair of copper(II) ions have 4 + 1 coordination while the outer pair have a distorted-tetrahedral geometry. The central pair are joined by two symmetrical Cu–Cl–Cu bridges with bridging bond angles of 96.35° each. One symmetrical Cu–Cl–Cu bridge and one asymmetrical Cu–Cl···Cl bridge link each outer copper ion to a central ion. The bridging angles are 95.51 and 88.3°, respectively. The magnetic properties are indicative of a weak ferromagnetic interaction for both bridges, but the data did not allow specific values for the exchange coupling to be determined.

Introduction

The structural chemistry of copper(II) chlorides and bromides is extremely diverse as a result of that metal's flexible coordination geometry coupled with the bridging capability of the halide ions. The former characteristic leads to situations where two or more coordination geometries coexist within a structure, e.g., square pyramidal and distorted tetrahedral in $[C_6H_{18}N_3]_4Cu_5Cl_{22}$,[2] tetrahedrally distorted 4 + 1 and 4 + 2 geometries in $[(CH_3)_2CHNH_3]_2CuCl_4$,[3] and distorted tetrahedral and 4 + 2 geometry in $[(C_2H_5)_2NH_2]_2Cu_4Br_{10}\cdot EtOH$.[4] The relative flatness of the potential surface defining the coordination geometry is further seen by the ability of the square-pyramidal $CuCl_5^{3-}$ ion in $M(NH_3)_6CuCl_5$ salts[5] to undergo dynamic reorientation of its C_4 axis. The ability to transform between coordination geometries is demonstrated by the phenomenon of thermochromism,[6] in which the stereochemistry changes as materials pass through structural phase transitions.

The capability of the halides to act as bridging ligands between copper ions leads to a variety of oligomeric and polymeric species. In a recent review,[7] we summarized the findings on $ACuCl_3$ salts. These included structures containing isolated $Cu_2Cl_6^{2-}$ ions, stacks of $Cu_2Cl_6^{2-}$ ions linked by semicoordinate linkages, bibridged chains with square-pyramidal coordination geometry, and tribridged chains with 4 + 2 coordination geometry. In particular, we argued that the presence of bulky, non-hydrogen-bonding

---

(1) Current address: Chemistry Division, Argonne National Laboratory, Argonne, IL 60439.

(2) Antolini, L.; Marcotrigiano, G.; Menabue, L.; Pellacani, G. C. *J. Am. Chem. Soc.* **1980**, *102*, 5506.

(3) Anderson, D. N.; Willett, R. D. *Inorg. Chim. Acta* **1974**, *8*, 167. Bloomquist, D. R.; Willett, R. D.; Dodgen, H. W. *J. Am. Chem. Soc.* **1981**, *103*, 2610.

(4) Fletcher, R.; Hansen, J. J.; Livermore, J.; Willett, R. D. *Inorg. Chem.* **1983**, *22*, 330.

(5) Reinen, D.; Friebel, C. *Inorg. Chem.* **1984**, *23*, 791.

(6) Bloomquist, D. R.; Willett, R. D. *Coord. Chem. Rev.* **1982**, *47*, 125.

(7) Willett, R. D.; Geiser, U. *Croat. Chem. Acta* **1984**, *57*, 737.